ACS OMEGA

http://pubs.acs.org/journal/acsodf

Article

Superior Sensitivity and Optical Response of Blue Phosphorene and Its Doped Systems for Gas Sensing Applications

Fatemeh Safari, Mahdi Moradinasab,* Udo Schwalke, and Lado Filipovic

Cite This: *ACS Omega* 2021, 6, 18770−18781

Read Online

ACCESS | Metrics & More | Article Recommendations

ABSTRACT: The first-principles calculation of pristine, B-, Al-, Ga-, Sb-, and Bi-doped blue phosphorene (BlueP) with adsorbed SO_2, NO, and NO_2 gas molecules including the transport and optical properties is reported. The electronic structures of pristine and doped BlueP are investigated, and the modifications in electronic band structures and density (DOS) of states are studied. The most considerable adsorption energies of BlueP after being exposed to paramagnetic gas molecules NO and NO_2 show excellent sensitivity to the considered gas molecules, which is confirmed by the current−voltage characteristics. The pristine and doped BlueP can be encouraging alternatives for new-generation optical gas sensors due to notable alterations in the pristine and doped BlueP optical spectra.

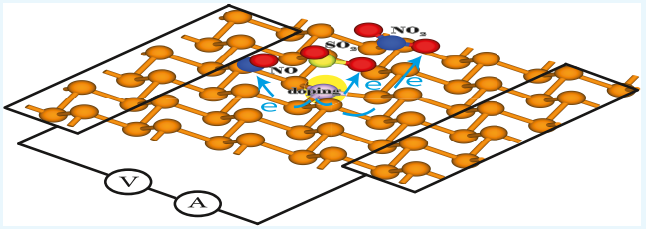

INTRODUCTION

Gas sensors play an important role in modern society to ensure safety, health, and environmental reservation.[1] Increasing environmental pollution from factory waste and the need to quickly identify toxic gases have boosted fundamental research in material science and physics of novel materials, which can provide sufficient sensitivity at room temperature. To detect gas molecules in stable environmental situations, at room temperature, and to attain high sensibility and selectivity, new materials are utilized in gas sensors.[2] Two-dimensional (2D) materials have attracted strong interest owing to their irreplaceable electronic, spintronic, and optoelectronic properties. Besides, the leading characteristics of 2D materials, such as their excellent response and sensibility, in particular, their reasonable price and lack of complexity in manufacturing, result in comprehensive utilization in gas detection applications.[2,3]

Graphene and transition-metal dichalcogenides (e.g., MoS_2, WSe_2) are the most commonly investigated 2D materials and have attracted attention in recent years. However, the lack of a band gap in graphene[4,5] and the low room-temperature carrier mobility in MoS_2[6] have limited the real-world applicability of these materials.

Phosphorene[7] (also known as black phosphorene) is a new and emerging 2D material with myriad applications based on theoretical and experimental studies.[7] Phosphorene[8,9] has a vertically corrugated structure of phosphorus atoms in a single layer.[10] A new allotrope of black phosphorene named blue phosphorene (BlueP), which contains a more flatly single layer of phosphorus atoms,[10] was first reported by Zhu et al.[11] Moreover, Zhang et al.[12] synthesized monolayer BlueP on Au(111) using molecular beam epitaxial in 2016. Similar to black phosphorene, BlueP is a semiconductor with high carrier mobility (over 1000 $cm^2\ V^{-1}\ s^{-1}$),[13] which can be higher than various common 2D semiconductors, such as MoS_2 (around 200 $cm^2\ V^{-1}\ s^{-1}$).[14]

BlueP has an indirect and fundamental wide band gap of about 2 eV at the Perdew−Burke−Ernzerhof (PBE) level.[11,15] However, due to the breaking of bond symmetry in BlueP, Dirac points can be easily distorted by introducing dopants. As a result, the indirect band gap of BlueP can be modified to a direct band gap by doping, as further described in this paper.

Besides the aforementioned outstanding properties of the new 2D gas sensing materials, they have a high surface-to-volume ratio, obvious charge transfers from host 2D materials to gas molecules, and tunable functionality of the surface[16,17] for decoration species as structural merits. The gas molecule adsorption modifies the conductivity by imposing charge donors/acceptors, which is employed as a gas sensing mechanism. It is predicted that the gas molecule adsorption can influence the electrical conductivity of BlueP,[18] thus showing that conductivity variations can improve the gas concentration detection. On the other hand, the optical responses of BlueP in the presence of gas molecules exhibit a distinct detection method compared to alternative 2D materials such as graphene, MoS_2, $MoSe_2$, and WS_2. Substitutional doping can act as a powerful tool to modify the electronic, optical, and

Received: April 9, 2021
Accepted: June 29, 2021
Published: July 13, 2021

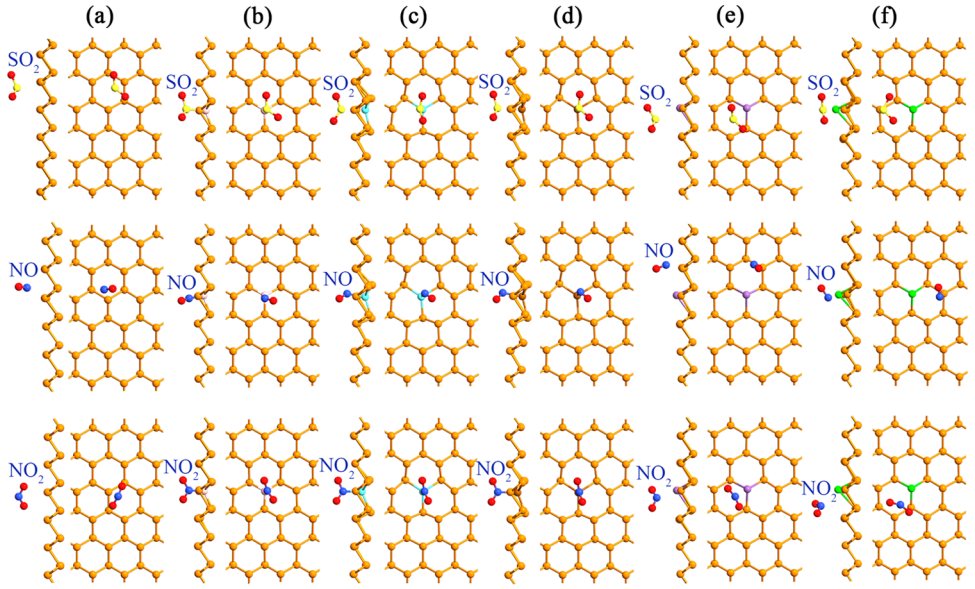

Figure 1. Top and side views of the fully relaxed structure (a) BlueP, (b) BlueP-B, (c) BlueP-Al, (d) BlueP-Ga, (e) BlueP-Sb, and (f) BlueP-Bi for the adsorbed SO_2, NO, and NO_2 gas molecules. The Al, B, Bi, Ga, and Sb atoms are indicated in cyan, pink, green, brown, and violet colors, respectively.

Table 1. Adsorption Energy (E_{ads}), Charge Transfer (ΔQ), Adsorption Distance (d), and Band Gap (E_g) of Gas Molecules on Pristine BlueP and Its Doped Systems

		SO_2				NO				NO_2			
substrate	E_g (eV)	E_{ads} (eV)	ΔQ (e)	d (Å)	E_g (eV)	E_{ads} (eV)	ΔQ (e)	d (Å)	E_g (eV)	E_{ads} (eV)	ΔQ (e)	d (Å)	E_g (eV)
pristine BlueP	1.93	−0.17	0.17	2.42	1.67	−0.22	0.21	1.78	0.65	−0.48	0.19	2.43	0.71
B-doped BlueP	1.43	−0.46	0.49	1.31	0.80	−1.37	0.90	0.89	0.75	−1.05	1.07	0.99	0.11
Al-doped BlueP	1.62	−0.45	0.44	1.20	0.59	−1.04	0.64	0.68	0.77	−1.08	0.95	1.08	1.50
Ga-doped BlueP	1.60	−0.26	0.49	1.17	0.86	−0.77	0.51	0.60	0.64	−0.83	0.86	1.09	1.49
Sb-doped BlueP	1.73	−0.06	0.13	2.54	1.38	−0.20	0.28	1.09	0.41	0.00	0.26	2.09	0.50
Bi-doped BlueP	1.59	−0.25	0.50	1.48	1.52	−0.21	0.38	1.10	0.52	−0.01	0.26	1.80	0.35

magnetic properties and also the gas sensing operation of 2D substances.[19−22] According to first-principles studies, changes in the electronic and transport features after the adsorption of gas molecules such as NO_2, NO, and NH_3 prove the high capacity of BlueP,[20,21,23,24] as a gas sensor material. Although the role of BlueP as a gas sensing material is investigated theoretically in some research, the study on the impact of such gas molecules on the optical properties of BlueP and its doped system is still lacking.

Here, we explore the conductivity and optical sensing properties of pristine, B-, Al-, Ga-, Sb-, and Bi-doped BlueP with regard to the adsorption of three gas molecules: SO_2, NO, and NO_2. The adsorption process is investigated by calculating adsorption features such as adsorption energy, adsorption distance, and charge transfer. The density functional theory (DFT) calculations demonstrate that the transmission and optical spectrum of BlueP can be modified significantly by the above-mentioned gas molecules. The pristine and doped BlueP substrates are encouraging candidates to develop new-generation gas sensors.

RESULTS AND DISCUSSION

First, to confirm the accuracy of our results, the structural and electronic properties of pristine BlueP are investigated. The results indicate that the optimized lattice constant, bond length, and buckling height (h) of pristine BlueP are 3.27, 2.27, and 1.26 Å, respectively. After substituting B, Al, Ga, Sb, and Bi impurities in pristine BlueP, all doped BlueP structures are entirely relaxed. The compatibility of results with literature findings is good.[19,25,26] To estimate the possibility of the experimental synthesis of the doped substrates, the cohesive energy (E_{coh}) is calculated.[27] Cohesive energies of −0.18, −0.11, −0.09, −0.12, and −0.11 eV per atom are achieved for B-, Al-, Ga-, Sb-, and Bi-doped BlueP substrates, respectively. The obtained cohesive energies prove the stability of the considered substrates. The bond lengths of the considered gas molecules are set to 1.47, 1.17, and 1.21 Å for SO_2, NO, and NO_2 in simulations, respectively. For SO_2, the O−S−O angle is 119.99°, while the O−N−O angle for NO_2 is 133.67°.[28] For each adsorption case, the gas molecule is located near the substrate, and the entire system is again completely relaxed. The top and side views of the entirely relaxed structures for the adsorbed SO_2, NO, and NO_2 molecules are shown in Figure 1. The corresponding adsorption energies and adsorption distances are listed in Table 1. Based on the definition of E_{ads}, a negative value denotes that the adsorption of gas molecules on the substrate is favorable energetically.[29] In addition, a smaller distance between the substrate and the gas molecule can indicate a stronger interaction (Figures 2 and 3).[29] To further study the dynamic stability of doped BlueP at 300 K, Ab Initio Molecular Dynamics (AIMD) simulations are implemented. The canonical NVT ensemble is used; moreover, the simulation time and time step are set to be 1.0 ps and 1.0 fs, respectively. We find that the

https://doi.org/10.1021/acsomega.1c01898
ACS Omega 2021, 6, 18770−18781

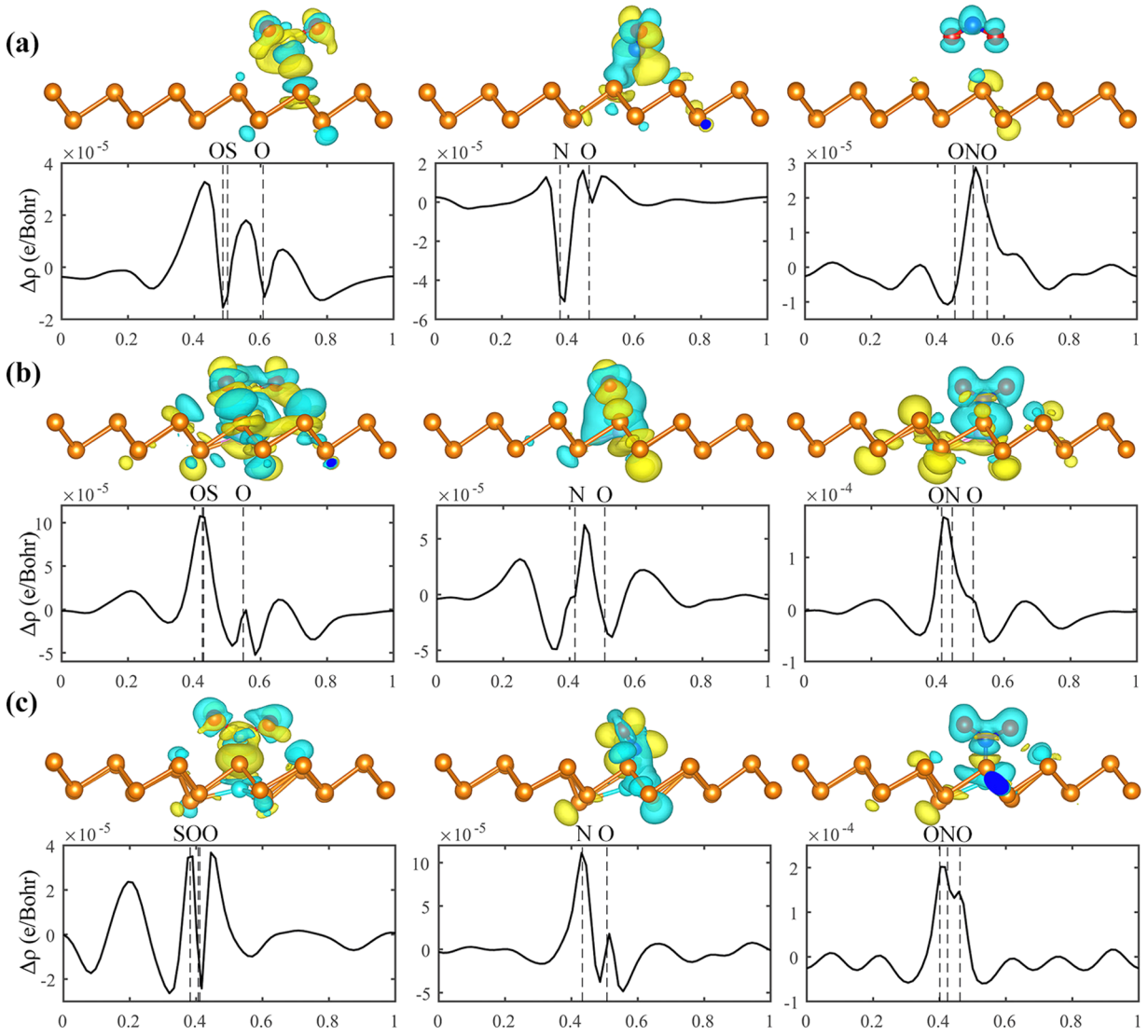

Figure 2. Plane-averaged charge density difference and the side views of the charge density difference of (a) BlueP, (b) BlueP-B, and (c) BlueP-Al for the adsorbed SO_2, NO, and NO_2 gas molecules along the z-direction. The yellow and blue isosurfaces represent electron accumulation and depletion, respectively. The vertical dashed lines indicate the positions of the N, O, and S atoms in the structures.

pristine and doped BlueP are dynamically stable at 300 K during the entire simulation time (t = 1.0 ps).

Pristine BlueP. As shown in Figure 1a, after full relaxation, the sulfur, nitrogen, and oxygen atoms in the SO_2, NO, and NO_2 molecules, respectively, are sited in the buckled honeycomb structure. The adsorption distances of 2.42, 1.78, and 2.43 Å are observed for SO_2, NO, and NO_2, respectively (see Table 1). Of the three gas molecules, SO_2 exhibits the smallest adsorption energy (−0.17 eV) and charge transfer (0.17e). The adsorption of NO induces great adsorption energy (−0.22 eV) and the largest charge transfer (0.21e) among the three considered gas molecules, indicating that the pristine BlueP monolayer is sensitive to NO. The pristine BlueP demonstrates a high sensitivity to NO_2 molecules with the largest adsorption energy (−0.48 eV) and relatively large charge transfer (0.19e). Therefore, the pristine BlueP film may be sufficient for the detection of NO and NO_2 gases, but may not be ideal for SO_2. The effect of gas adsorption on the electronic band structures of pristine BlueP is further studied, as shown in Figure 4. The pristine BlueP semiconductor has an indirect band gap of 1.93 eV, which is the vertical distance between the conduction band minimum (CBM) placed along the Γ−Y line and the valence band maximum (VBM) located at the midpoint of the region along the T−Z line.[11,19] The adsorption of SO_2, NO, and NO_2 reduces the band gap of pristine BlueP to 1.67, 0.65, and 0.71 eV, respectively. As a result of the spin-splitting bands with NO and NO_2 adsorption, the indirect band gap of pristine BlueP is smaller when exposed to NO and NO_2 gas molecules than SO_2. As a further investigation, the total density of states (TDOS) and projected density of states (PDOS) of pristine BlueP are computed before and after the molecular adsorption. The adsorption of the SO_2 gas molecule brings about a new defect peak at about −0.70 eV in the DOS (see Figure 4b). According to the paramagnetic nature of NO and NO_2 gas molecules, the adsorption of these gases on pristine BlueP creates significant modifications in the DOS close to the Fermi level, and these gas adsorptions lead to a magnetic moment of 1 μB. The adsorbed NO molecule brings about a spin-up defect state at about −0.34 eV (see Figure 4c). However, the adsorption of NO_2 induces two peaks in the band gap that these spin states are dissimilar, as illustrated in Figure 4d. The results shown here agree with previous studies in an utterly convincing way.[21,23]

https://doi.org/10.1021/acsomega.1c01898
ACS Omega 2021, 6, 18770−18781

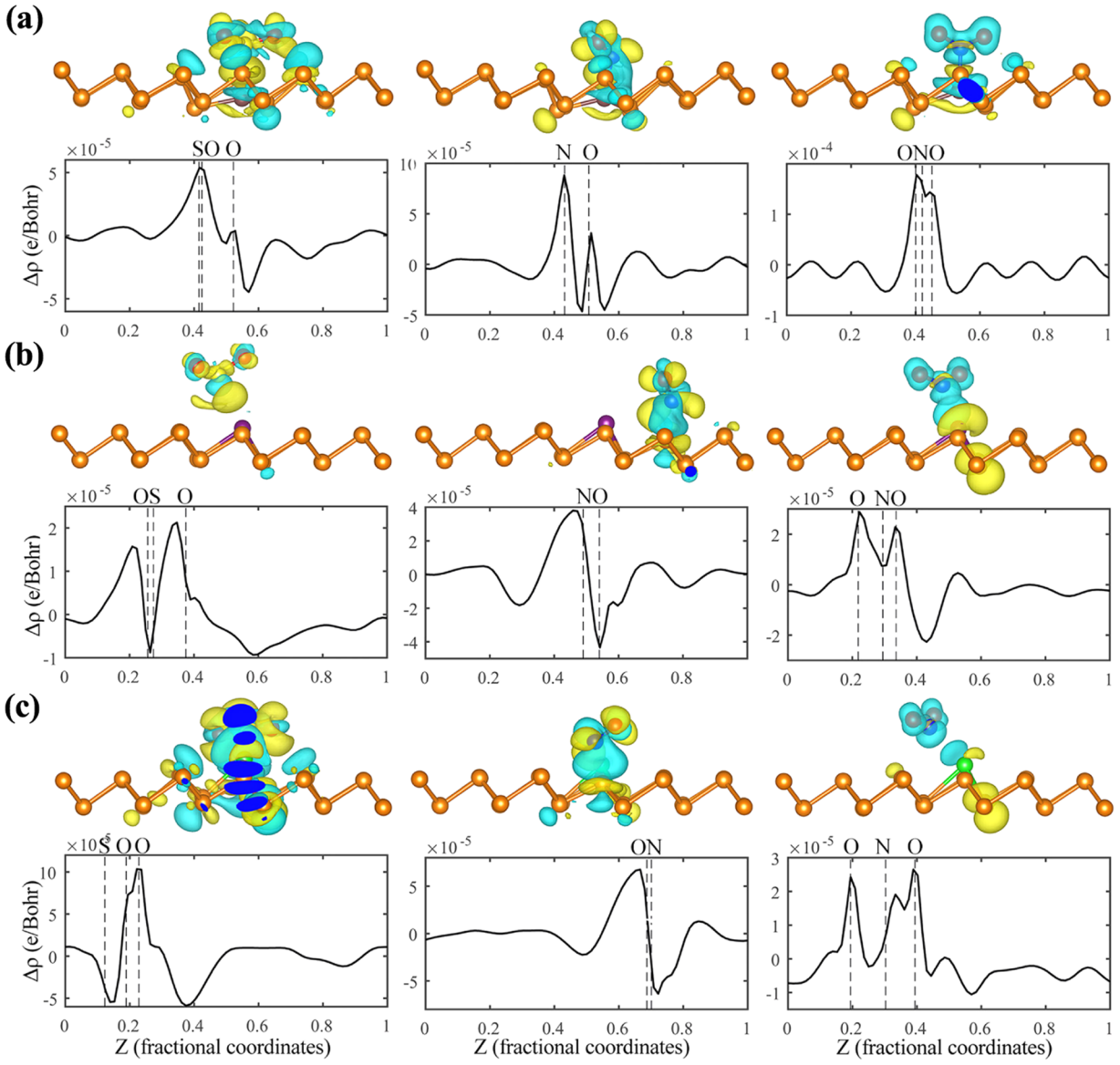

Figure 3. Plane-averaged charge density difference and the side views of the charge density difference of (a) BlueP-Ga, (b) BlueP-Sb, and (c) BlueP-Bi for the adsorbed SO_2, NO, and NO_2 gas molecules along the *z*-direction. The yellow and blue isosurfaces represent electron accumulation and depletion, respectively. The vertical dashed lines indicate the positions of the N, O, and S atoms in the structures.

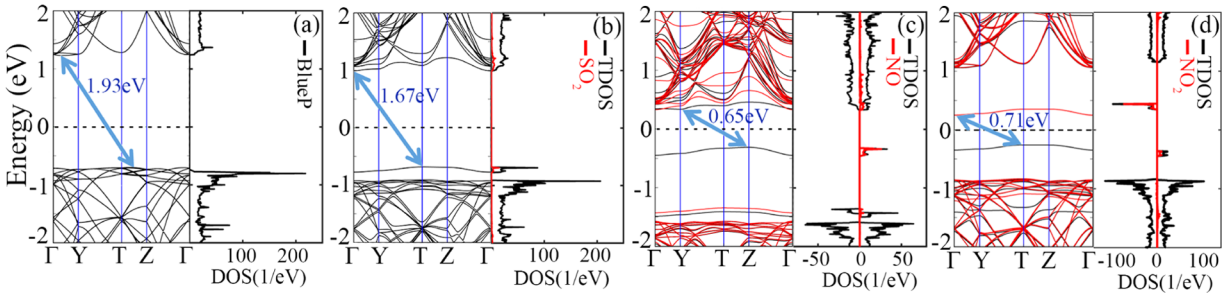

Figure 4. Band-gap structure, total density of states (TDOS), and projected density of states (PDOS) of BlueP (a) before and after (b) SO_2, (c) NO, and (d) NO_2 adsorption. The Fermi energy indicated by a black dashed line is set to zero. Red lines present spin-down in band gap diagrams. The positive and negative values represent spin-up and spin-down states, respectively.

B-Doped BlueP. The obtained adsorption distances for SO_2, NO, and NO_2 molecules adsorbed on B-doped BlueP substrates are 1.31, 0.89, and 0.99 Å, respectively. According to the calculated sum of covalent atomic radii of B−S (1.88 Å) and B−N (1.56 Å),[30] the formation of a chemical bond between the considered gas molecules and the B-doped BlueP substrate is expected (see Figure 1b). The calculations show that E_{ads} is extremely affected by the boron dopant (Table 1). Compared

https://doi.org/10.1021/acsomega.1c01898
ACS Omega 2021, 6, 18770−18781

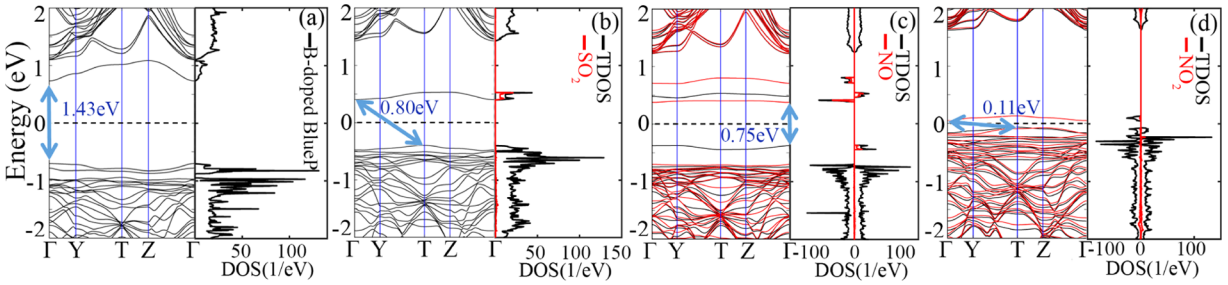

Figure 5. Band gap structure, total density of states (TDOS), and projected density of states (PDOS) of B-doped BlueP (a) before and after (b) SO_2, (c) NO, and (d) NO_2 adsorption. The Fermi energy indicated by a black dashed line is set to zero. Red lines present spin-down in band gap diagrams. The positive and negative values represent spin-up and spin-down states, respectively.

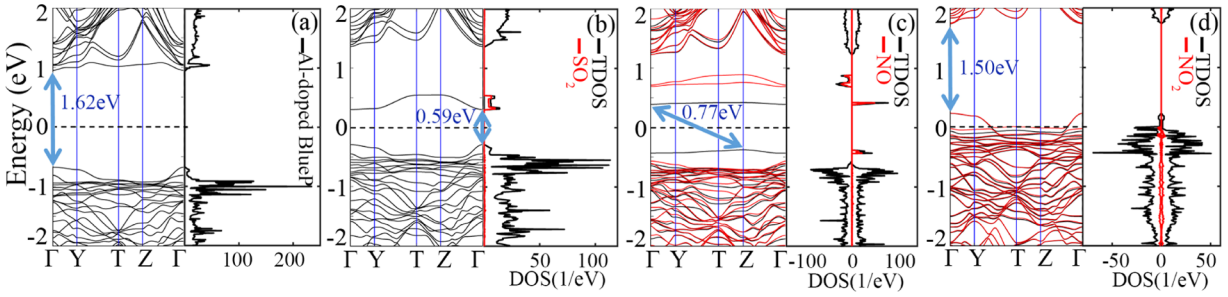

Figure 6. Band gap structure, total density of states (TDOS), and projected density of states (PDOS) of Al-doped BlueP (a) before and after (b) SO_2, (c) NO, and (d) NO_2 adsorption. The Fermi energy indicated by a black dashed line is set to zero. Red lines present spin-down in band gap diagrams. The positive and negative values represent spin-up and spin-down states, respectively.

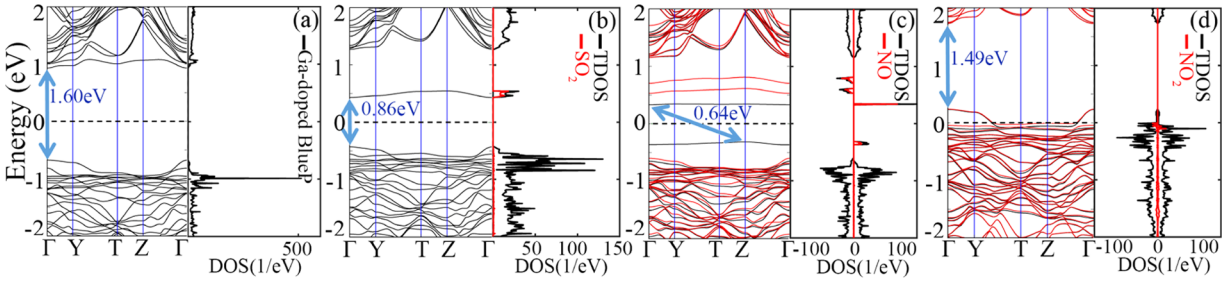

Figure 7. Band gap structure, total density of states (TDOS), and projected density of states (PDOS) of Ga-doped BlueP (a) before and after (b) SO_2, (c) NO, and (d) NO_2 adsorption. The Fermi energy indicated by a black dashed line is set to zero. Red lines present spin-down in band gap diagrams. The positive and negative values represent spin-up and spin-down states, respectively.

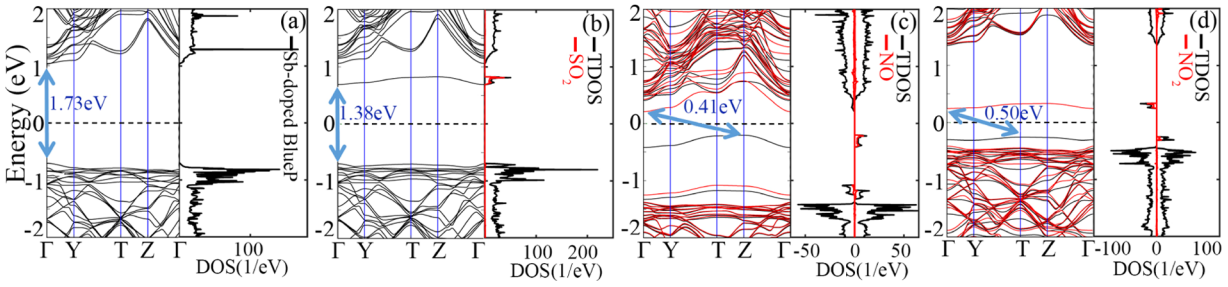

Figure 8. Band gap structure, total density of states (TDOS), and projected density of states (PDOS) of Sb-doped BlueP (a) before and after (b) SO_2, (c) NO, and (d) NO_2 adsorption. The Fermi energy indicated by a black dashed line is set to zero. Red lines present spin-down in band gap diagrams. The positive and negative values represent spin-up and spin-down states, respectively.

with the pristine BlueP, the adsorption energies of SO_2, NO, and NO_2 on B-doped BlueP increase to −0.46, −1.37, and −1.05 eV, respectively. Noticeable charge transfers of 0.49*e*, 0.90*e*, and 1.07*e* are achieved from the B-doped BlueP system after exposure to SO_2, NO, and NO_2, respectively. As displayed in Figures 5a, 6a, 7a, 8a, and 9a, the band gap of the pristine BlueP is reduced after substitutional doping. In the B-doped system, the VBM and CBM are shifted to the Γ point, making it a direct-gap semiconductor with a band gap of near 1.43 eV. The adsorption of SO_2, NO, and NO_2 reduces the direct band gap of B-doped BlueP to 0.80, 0.75, and 0.11 eV, respectively. As a consequence of the spin-splitting bands, the direct band gap of

https://doi.org/10.1021/acsomega.1c01898
ACS Omega 2021, 6, 18770−18781

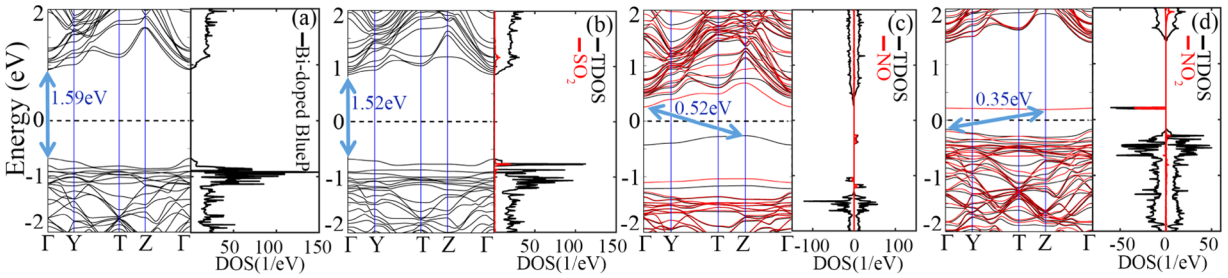

Figure 9. Band gap structure, total density of states (TDOS), and projected density of states (PDOS) of Bi-doped BlueP (a) before and after (b) SO_2, (c) NO, and (d) NO_2 adsorption. The Fermi energy indicated by a black dashed line is set to zero. Red lines present spin-down in band gap diagrams. The positive and negative values represent spin-up and spin-down states, respectively.

B-doped BlueP is decreased when being exposed to NO_2 gas molecules, as shown in Figure 5. The TDOS of the B-doped BlueP substrate before gas adsorption is presented in Figure 5a. The adsorption of the SO_2 molecule brings about a sharp peak at around 0.53 eV in the TDOS (Figure 5b). Similar to pristine BlueP, the paramagnetic nature of NO and NO_2 molecules produces a magnetic moment of 1 μB. The NO molecule induces some spin-up and spin-down states, as shown in Figure 5c. Furthermore, there are apparent changes in the DOS close to the Fermi level for the adsorbed NO_2 (see Figure 5d).

Al-Doped BlueP. Adsorption distances of 0.68 and 1.08 Å are calculated for the Al-doped BlueP in the presence of NO and NO_2 gas molecules. These small adsorption distances result in chemisorption and forming chemical bonds due to the large sum of atom covalent radii Al−N (1.97 Å). Although the nearest vertical distance for the SO_2 molecule has a smaller value than the equivalent sum of covalent atomic radii (2.29 Å), owing to the considerable spatial distance (2.49 Å), the chemical bond is not formed (Figure 1c and Table 1). From the calculations, given in Table 1, E_{ads} is extremely affected by the aluminum dopant. The adsorption energies of SO_2, NO, and NO_2 on Al-doped BlueP increase to −0.45, −1.04, and −1.08 eV, respectively, compared to the pristine BlueP. The large charge transfers of 0.44*e*, 0.64*e*, and 0.95*e* from the Al-doped BlueP substrate to the SO_2, NO, and NO_2 gas molecules are obtained, respectively. Doping with an Al impurity induces a transition from an indirect- to a direct-gap semiconductor with a band gap of nearly 1.62 eV. Similar to the B-doped BlueP, the VBM and CBM are sited at the Γ point. The adsorption of SO_2, NO, and NO_2 reduces the band gap of Al-doped BlueP to 0.59, 0.77, and 1.50 eV, respectively (see Figure 6b−d). The direct band gap of the Al-doped BlueP system remains unchanged when it is exposed to SO_2 and NO_2; however, the system exhibits a direct- to indirect-band-gap transition through NO adsorption. The TDOS of the Al-doped BlueP structure before gas adsorption is shown in Figure 6a. The adsorption of SO_2 leads to several states on a narrow energy bound of 0.30−0.54 eV above the Fermi level, as displayed in Figure 6b. However, the adsorption of paramagnetic molecules NO and NO_2 induces magnetic moments of 1 and 0.26 μB, respectively. The adsorption of NO gas molecule induces some spin-up and -down states in the gap (see Figure 6c). Furthermore, the adsorption of the NO_2 molecule brings about unoccupied local states in the valence band and results in p-type semiconducting behavior by moving the Fermi level into the original valence bands (Figure 6d).

Ga-Doped BlueP. Adsorption distances of 0.60 and 1.09 Å are calculated for the Ga-doped BlueP in the presence of NO and NO_2 gas molecules, respectively. These are remarkably lesser than the sum of the atom covalent radii Ga−N (1.95 Å). Therefore, chemisorption occurs and a chemical bond is formed. For SO_2 gas molecule adsorption, the nearest vertical distance is small compared to the sum of covalent atomic radii (2.27 Å). However, the spatial distance remains 2.53 Å (see Figure 1d and Table 1). Therefore, as was the case with the Al-doped system, no chemical bonds are expected to form. The adsorption energies of NO and NO_2 on Ga-doped BlueP structures are significantly greater than pristine BlueP due to the covalent bond formation between the Ga and N atoms. In addition, the adsorption energy of SO_2 on Ga-doped BlueP increases to −0.26 eV (see Table 1). The amounts of charge transferred from the Ga-doped BlueP to SO_2, NO, and NO_2 are 0.49*e*, 0.51*e*, and 0.86*e*, respectively. As shown in Figure 7a, doping with a Ga impurity causes the transition from an indirect- to a direct-gap semiconductor with a band gap of nearly 1.60 eV, similar to that observed with Al doping, with the VBM and CBM once again at the Γ point. The adsorption of SO_2, NO, and NO_2 reduces the band gaps of Ga-doped BlueP to 0.86, 0.64, and 1.49 eV, respectively (see Figure 7b−d). The direct-band-gap characteristic of this substrate remains unchanged after SO_2 and NO_2 adsorption, while the Ga-doped BlueP exhibits a direct to indirect-band-gap transition by NO adsorbent. The TDOS of the Ga-doped BlueP substrate before gas adsorption is shown in Figure 7a. The SO_2 adsorption leads to some defect states within the bounds of 0.43−0.55 eV above the Fermi level (see Figure 7b). However, the paramagnetic nature of NO and NO_2 gas molecules leads to a magnetic moment of 1 and 0.22 μB, respectively. As shown in Figure 7c, the NO molecule adsorption induces some spin-up and spin-down states in the gap. Furthermore, the adsorption of the NO_2 molecule brings about unoccupied local states in the valence band and results in p-type semiconducting behavior by moving the Fermi level into the original valence bands (Figure 7d).

Sb-Doped BlueP. The sulfur atom of SO_2 is fixed at the middle of the buckled honeycomb, while the NO molecule is sited at the bridge of the P−P bond after complete relaxation. The nitrogen atom of NO_2 is situated in the buckled honeycomb (see Figure 1e). Adsorption distances of 2.54, 1.09, and 2.09 Å are obtained for the SO_2, NO, and NO_2 gas molecules adsorbed on Sb-doped BlueP substrate, respectively (see Table 1). The nearest distance for the SO_2 gas molecule is greater than the covalent atomic radii of Sb−S (2.43 Å). Moreover, although the vertical distances for the NO and NO_2 molecules have a smaller value than the equivalent sum of covalent atomic radii, the spatial distances are 2.12 and 2.55 Å, respectively, as given in Figure 1e. Therefore, this system should result in no chemical bond formation. As shown in Table 1, the adsorption energies of the Sb-doped BlueP system are little compared to pristine BlueP. The amount of charge transfer for NO is 0.28*e*, which is larger

https://doi.org/10.1021/acsomega.1c01898
ACS Omega 2021, 6, 18770−18781

Table 2. Impacts of Adsorption of Different Gas Molecules on the Conductivity of Pristine BlueP and Its Doped Systems

substrate	SO_2	NO	NO_2
pristine BlueP	the decrease in conductivity, the lowest current level at 3^V	the dramatic increase in conductivity ($2.4-3^V$)	the sharp increase in conductivity ($2-3^V$), the highest current level at 3^V
B-doped BlueP	the increase in conductivity ($2-3^V$), the lowest current level at 3^V	the increase in conductivity ($2.4-3^V$)	the dramatic increase in conductivity ($1.2-3^V$), the highest current level at 3^V
Al-doped BlueP	the increase in conductivity, the highest current level at 3^V	the increase in conductivity	the increase in conductivity, the lowest current level at 3^V
Ga-doped BlueP	the decrease in conductivity, the lowest current level at 3^V	the sharp increase in conductivity ($2-2.4^V$), the highest current level at 3^V	the increase in conductivity
Sb-doped BlueP	the decrease in conductivity, the lowest current level at 3^V	NDR ($2.4-2.6^V$), the increase in conductivity	the dramatic increase in conductivity, the highest current level at 3^V
Bi-doped BlueP	the increase in conductivity, the lowest current level at 3^V	the sharp increase in conductivity ($1.8-2.6^V$)	the increase in conductivity, the highest current level at 3^V

Table 3. Current Value, Current Ratio, and Sensitivity of Pristine BlueP and Its Doped Systems at Voltage Bias of 3 V

	SO_2			NO			NO_2		
substrate	I (μA)	current ratio	sensitivity (%)	I (μA)	current ratio	sensitivity (%)	I (μA)	current ratio	sensitivity (%)
pristine BlueP	17.56	0.96	3.83	26.80	1.47	46.77	28.62	1.57	56.74
B-doped BlueP	27.18	1.30	30.11	33.22	1.59	59.02	38.28	1.83	83.25
Al-doped BlueP	21.90	1.63	62.70	17.20	1.28	27.79	15.65	1.16	16.27
Ga-doped BlueP	11.10	0.88	13.60	17.47	1.39	38.54	17.37	1.38	37.75
Sb-doped BlueP	9.73	0.94	5.63	11.95	1.16	15.91	19.47	1.89	88.85
Bi-doped BlueP	13.16	1.15	14.93	17.41	1.52	52.05	18.34	1.60	60.17

than those for NO_2 and SO_2. As shown in Figure 8a, doping with a Sb impurity results in a transition from an indirect- to a direct-gap semiconductor with a band gap of nearly 1.73 eV at the Γ point. The adsorption of SO_2, NO, and NO_2 reduces the band gap of Sb-doped BlueP to 1.38, 0.41, and 0.50 eV, respectively (see Figure 8b−d). The direct-band-gap characteristic of this substrate remains unchanged after SO_2 adsorption, while a direct to indirect-band-gap transition occurs by NO and NO_2 adsorbent. The TDOS of the Sb-doped BlueP structure before gas molecule adsorption is displayed in Figure 8a. The adsorption of SO_2 leads to several defect states within the energy bounds of 0.69−0.83 eV above the Fermi level, as shown in Figure 8b. However, the paramagnetic nature of NO and NO_2 gas molecules leads to a magnetic moment of 1 μB and significant modifications around the Fermi level in the DOS. The adsorbed NO gives rise to one spin-up defect state at about −0.22 eV (see Figure 8c). Furthermore, the adsorption of NO_2 induces two peaks in the band gap, corresponding to different spin states, as illustrated in Figure 8d.

Bi-Doped BlueP. After complete relaxation, the sulfur atom from the SO_2 molecule is fixed at the top of the P atom, while the nitrogen atom from the NO and NO_2 molecules is sited in the buckled honeycomb (see Figure 1f). The obtained results for the SO_2, NO, and NO_2 gas molecules show the adsorption distances of 1.48, 1.10, and 1.80 Å, respectively (see Table 1). Although the nearest vertical distance for the studied gas molecules is smaller than their atomic radii, the spatial distances are 2.46, 2.06, and 2.90 Å, respectively, indicating that the formation of a chemical bond between the considered gas molecules and the Bi-doped BlueP substrate is unexpected. The SO_2 adsorption energy on the Bi-doped BlueP is larger than the pristine BlueP. However, the adsorption energy of NO and NO_2 on Bi-doped BlueP decreases to −0.21 and −0.01 eV, respectively (see Table 1). The amount of charge transfer changed for the cases of NO and NO_2 adsorption to 0.38e and 0.26e, respectively, which is smaller than that of SO_2. Doping with a Bi impurity results in an indirect- to a direct-gap transition with the amount of nearly 1.59 eV at the Γ point (see Figure 9a). Furthermore, the adsorption of SO_2, NO, and NO_2 reduces the band gap of Bi-doped BlueP to 1.52, 0.52, and 0.35 eV, respectively (see Figure 9b−d). Although the direct-band-gap characteristic of this substrate remains unchanged in the presence of SO_2 adsorbent, the Bi-doped BlueP exhibits a direct- to indirect-band-gap transition through NO and NO_2 adsorption. The TDOS of the Bi-doped BlueP structure before the adsorption of considered gas molecules is displayed in Figure 9a. The adsorption of SO_2 brings about a slight alteration around the Fermi level, as demonstrated in Figure 9b. However, the adsorption of paramagnetic NO and NO_2 gas molecules on Bi-doped BlueP leads to significant modifications in TDOS around the Fermi level. A magnetic moment of 1 μB is induced by the adsorption of these gas. The adsorbed NO causes one spin-up defect state at about −0.26 eV (see Figure 9c). The NO_2 adsorption results in a spin-down impurity state at about 0.20 eV in the band gap, as illustrated in Figure 9d.

***I*−*V* Characteristics.** The $I-V$ characteristic along the zigzag direction is calculated based on the nonequilibrium Green's function (NEGF) formalism to investigate the gas sensing operation of pristine BlueP and its doped structures. This measurement enables us to monitor the resistance variation in gas sensing materials. Furthermore, we can apply the $I-V$ curve and the resistance variation as a reference to compare with experimental measurements. Owing to the structural anisotropy of BlueP, it has two transport directions, including zigzag and armchair. It should be noted that we can disregard the resistance change induced by gas molecule absorption along the armchair direction due to its low current with 1 order of magnitude compared to the zigzag direction. Therefore, this section focuses on the electrical properties of BlueP in the zigzag direction. To elucidate a better understanding of the sensing performance, the sensitivity of BlueP and its doped systems is investigated. The sensitivity is calculated using $S\ (\%) = \frac{|G - G_0|}{G_0} \times 100\%$, where G_0 and G are the conductance of BlueP and its doped structures before and after gas molecule adsorption, respectively. We estimate the value using $G = ((I)/(V))$ at a potential bias of 3 V.

https://doi.org/10.1021/acsomega.1c01898
ACS Omega 2021, 6, 18770−18781

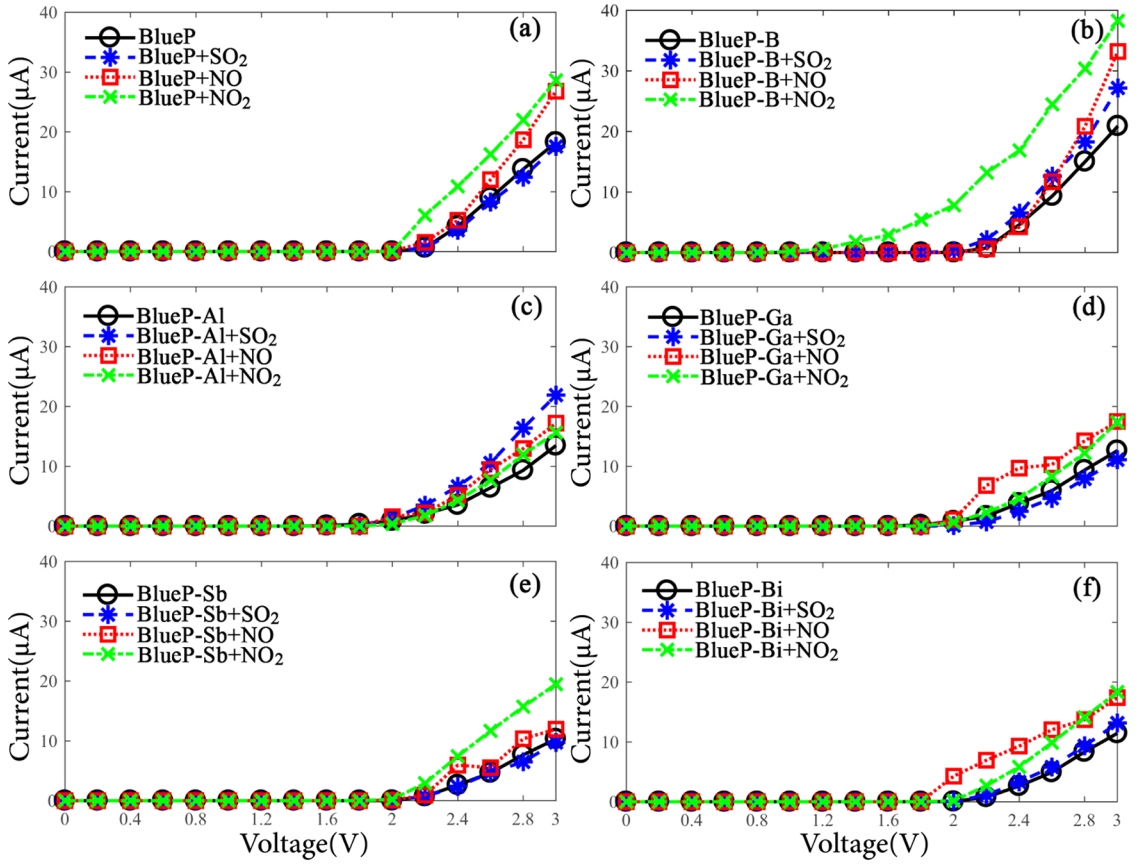

Figure 10. *I*−*V* characteristics along the zigzag direction of (a) pristine BlueP, (b) B-doped BlueP, (c) Al-doped BlueP, (d) Ga-doped BlueP, (e) Sb-doped BlueP, and (f) Bi-doped BlueP, before and after gas adsorption.

The current passing through the pristine BlueP structure is near 18.26 μA under a bias of 3 V. Nevertheless, after exposed to NO and NO_2 molecules, the current of BlueP can increase sharply to 26.80 and 28.62 μA under the same bias (see Tables 2 and 3). Therefore, after adsorption of these paramagnetic gas molecules, the conductivity increases dramatically compared to pristine BlueP (see Table 3). By contrast, the current decreases to 17.56 μA when the SO_2 gas molecule is adsorbed on the pristine BlueP. The sensitivity calculation of pristine BlueP also exhibits excellent sensing performance to NO_2 gas molecules (see Table 3). As displayed in Figure 10b, the chemical adsorption of SO_2, NO, and NO_2 on B-doped BlueP brings about an enlargement of the currents passing through it compared with that of a pristine BlueP. For NO_2 adsorbed, the least possible amount of voltage bias to induce noticeable current reduces from 2 to 1.2 V, which can be ascribed to spin defect states appearing at the band gap as observed in Figure 5d. Under a voltage bias of 3 V, the current passing from the B-doped BlueP region is 20.89 μA, which increases to 27.18, 33.22, and 38.28 μA when the substrate is exposed to SO_2, NO, and NO_2 gas molecules, respectively. When the applied bias is above 2.4 V, the current rises rapidly after the adsorption of NO gas molecule (see Tables 2 and 3). The current passing through the Al-doped BlueP sheet is smaller than pristine BlueP when exposed to NO and NO_2 gas molecules. Under a voltage bias of 3 V, the current passing from the Al-doped BlueP region is 13.46 μA, which increases to 21.90, 17.20, and 15.65 μA when the substrate is exposed to SO_2, NO, and NO_2 gas molecules. The induced change in current after gas molecule adsorption provides enough sensitivity to suggest excellent sensing performance, as summarized in Table 3. As shown in Figure 10c, upon SO_2 adsorption, the current along the zigzag direction is higher than other gas molecules under the bias of 3 V. Although B- and Al-doped BlueP structures have similar absorption energy for NO_2 gas molecules, this does not essentially lead to the same electrical conductivity response. Various parameters are effective in the electrical conductivity of the films, including charge transfer, band gap value, the states around the Fermi level, and asymmetry, which is induced by each impurity in the BlueP structure. In the case of the adsorbed NO_2 gas molecule on the Al-doped BlueP structure, as the calculations show, the adsorption distance is larger than that of the B-doped BlueP structure and the amount of the charge transfer and the magnetic moment are thereby also reduced. In addition, the band gap value does not change much compared to before gas absorption, and even the direct band gap is maintained. The DOS calculation also shows that, compared with the B-doped BlueP structure, the spin-down around the Fermi level is removed, which can reduce the current. In Figure 10d, we show the *I*−*V* curves of Ga-doped BlueP systems before and after gas molecule adsorption. The current 12.61 μA passes through the Ga-doped BlueP at the bias of 3 V, which is much lower than what is observed in pristine BlueP. The conductivity increases along the zigzag direction after NO and NO_2 adsorption, while it is reduced after SO_2 adsorption, as summarized in Tables 2 and 3. The reduction in current under SO_2 adsorption shows the increase in resistance of Ga-doped BlueP, which can be a direct measure of the sensitivity in the experiment. The conductivity along the zigzag direction increases dramatically when the NO_2 is adsorbed onto the Sb-doped BlueP. Although Sb-doped BlueP

https://doi.org/10.1021/acsomega.1c01898
ACS Omega 2021, 6, 18770−18781

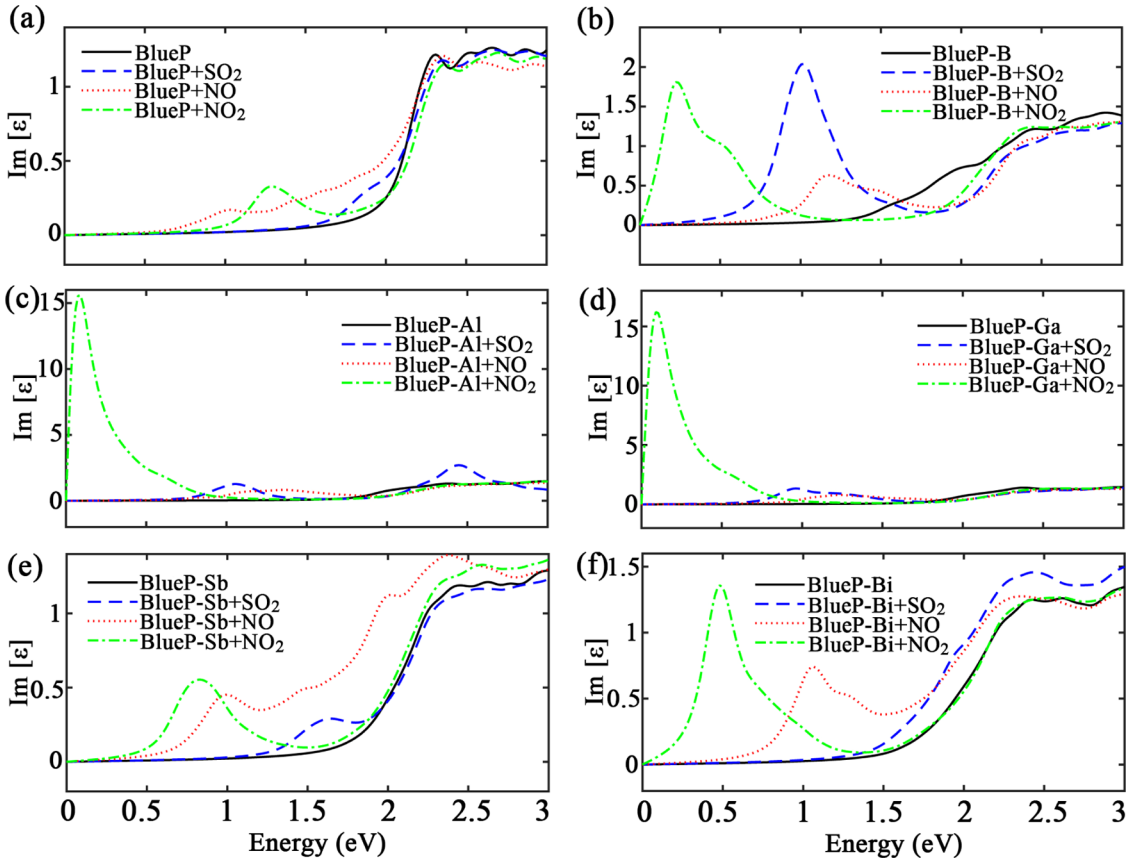

Figure 11. Imaginary part of the dielectric function versus the photon energy for (a) pristine BlueP, (b) B-doped BlueP, (c) Al-doped BlueP, (d) Ga-doped BlueP, (e) Sb-doped BlueP, and (f) Bi-doped BlueP, before and after gas adsorption.

structures have a small absorption energy for NO_2 gas molecules, this does not essentially lead to the low electrical conductivity response. As mentioned above, several parameters are influential in determining the electrical conductivity, including charge transfer, band gap value, the states around the Fermi level, and asymmetry, which is induced by each impurity in the BlueP structure. In the case of the adsorbed NO_2 gas molecule on the Sb-doped BlueP structure, as the results show, the amount of the charge transfer is large, and the magnetic moment is similar to pristine BlueP. In addition, the band gap value significantly changes compared to before gas absorption, and the DOS calculation also shows two peaks in the band gap, corresponding to different spins, as illustrated in Figure 8d. The rapid growth of current after the NO_2 adsorption can be ascribed to the appearance of spin states within the band gap. The current increases from 10.31 to 19.47 μA under the bias of 3 V (see Figure 10e). At the bias range of 2.4−2.6 V, a negative resistance behavior along the zigzag direction of Sb-doped BlueP is observed after exposure to NO gas molecule. It is observed that the current of the Sb-doped BlueP system reduces to 9.73 μA when exposed to the SO_2 gas molecule (see Tables 2 and 3). The current of the Bi-doped BlueP system is 11.45 μA at the voltage bias of 3 V, and it increases to 13.16, 17.41, and 18.34 μA when the substrate is exposed to SO_2, NO, and NO_2 gas molecules, respectively. At the voltage bias greater than 1.8 V, the current increases rapidly after the NO gas adsorption (see Figure 10f and Table 2). As summarized in Table 3, the Bi-doped BlueP exhibits high sensitivity to NO_2 gas molecules.

Optical Gas Sensing Properties. The optical gas sensors typically provide higher sensitivity and fast response in the real-time measurement, in contrast to the conductivity-based gas detectors.[31,32] Optical gas sensing properties can be evaluated from the frequency-dependent dielectric function which can be defined as $\epsilon(\omega) = \epsilon_1(\omega) + i\epsilon_2(\omega)$, where $\epsilon_1(\omega)$ and $\epsilon_2(\omega)$ are the real and imaginary components of $\epsilon(\omega)$, respectively. There is a direct relationship between the imaginary part of the dielectric function ($\mathrm{Im}[\epsilon]$) and the electronic band structure, which can determine the material's absorption properties.[33] To investigate the performance of BlueP and its doped structures as an optical gas sensor, the imaginary component of the dielectric function is computed by the Kramers−Kronig formula.[34] The imaginary component of the dielectric function for all substrates before and after the adsorption process is indicated in Figure 11. An extra peak is observed at lower energy than the first peak for all examined BlueP systems when they are exposed to NO or NO_2 molecules (see Table 4). In the pristine BlueP structure, the extra peak of NO_2 appears at a higher energy (1.29 eV) with a higher intensity compared to the NO gas molecule. However, the modification of dielectric function can be ignored by SO_2 exposure, as demonstrated in Figure 11a. As shown in Figure 11b, the imaginary part of the dielectric function for B-doped BlueP dramatically changes when exposed to the considered gas molecules. The presence of the NO_2 gas molecule near B-doped BlueP induces an additional peak at a lower energy than NO and SO_2. A new sharp peak is observed at about 1.02 eV in the imaginary part of the dielectric function for B-doped BlueP by SO_2 exposure. This peak is located at lower energies compared to B-doped BlueP, which shows the sensitivity of B-doped BlueP to SO_2 gas molecule in contrast to its $I-V$ characteristics. After SO_2 gas adsorption on the Al-doped BlueP system, two extra

https://doi.org/10.1021/acsomega.1c01898
ACS Omega 2021, 6, 18770−18781

Table 4. Impacts of Adsorption of Different Gas Molecules on the Absorption Spectrum of Pristine BlueP and Its Doped Systems

substrate	SO_2	NO	NO_2
pristine BlueP	insignificant effect	induces a new peak at 1.02 eV	induces a new peak at 1.29 eV
B-doped BlueP	induces a new peak at 1.02 eV	induces a new peak at 1.17 eV	induces a new peak at 0.23 eV
Al-doped BlueP	induces new peaks at 1.05 and 2.45 eV	induces a new peak at 1.35 eV	induces a new peak at 0.09 eV
Ga-doped BlueP	induces a new peak at 0.96 eV	induces a new peak at 1.23 eV	induces a new peak at 0.09 eV
Sb-doped BlueP	induces a new peak at 1.65 eV	induces a new peak at 0.99 eV	induces a new peak at 0.83 eV
Bi-doped BlueP	insignificant effect	induces a new peak at 1.07 eV	induces a new peak at 0.48 eV

peaks appear at 1.05 and 2.45 eV. The first peak of Al- and Ga-doped BlueP can be intensified sharply after NO_2 gas molecule adsorption (see Figure 11c,d). The adsorption of SO_2 and NO induces new peaks at 0.96 and 1.23 eV for the Ga-doped BlueP system, respectively; however, the intensity of the first peaks are smaller in comparison to the case of NO_2 adsorption (see Figure 11d). The presence of NO gas molecule near Sb-doped BlueP induces several additional peaks at a lower energy compared to the first peak. Furthermore, SO_2 gas molecules can lead to a new distinguished peak of about 1.65 eV at lower energies, which indicates a high sensitivity of this substrate to SO_2 gas molecules (Figure 11e). This detection is not observable in $I-V$ characteristics (see Figure 10). The adsorbed NO_2 induces the largest peak at 0.83 eV (see Figure 11e). As displayed in Figure 11f, for Bi-doped BlueP, an additional peak for NO appears at a higher energy (1.07 eV) with a smaller intensity than the NO_2 gas molecule. In contrast, the adsorption of SO_2 does not alter the optical absorption spectrum dramatically. Table 4 summarizes the changes in the absorption spectrum of BlueP and its doped structures in the presence of different gas molecules.

CONCLUSIONS

Based on the first-principles study, the electronic, transport, and optical properties of pristine and doped BlueP before and after SO_2, NO, and NO_2 gas molecules adsorption were investigated. DFT calculations reveal that the indirect band gap of BlueP shifts to a direct band gap by doping with B, Al, Ga, Sb, and Bi atoms. Transmission spectrum analysis indicates that the adsorption of considered gas molecules on pristine and doped BlueP is detectable. The current passing through BlueP and its doped systems can either decrease or increase after gas molecule adsorption, and these resistivity changes can be measured directly through experiments. The results show that B-doped BlueP can increase the sensitivity to SO_2, NO, and NO_2 gas molecules through strong chemical bonds. Moreover, Al- and Ga-doped BlueP can improve the sensitivity to the SO_2 gas molecule. On the other hand, Sb- and Bi-doped BlueP indicate an extraordinary sensitivity to NO and NO_2 gas molecules. Furthermore, these structures can be applied as sensing substances in the optical gas sensor based on dielectric function calculations. The presence of SO_2 in adjacent B- and Sb-doped BlueP considerably affects the dielectric functions, and a new peak emerges about 1.02 eV and 1.65 eV, respectively. These peaks indicate the high sensitivity of B- and Sb-doped BlueP to the presence of the SO_2 gas molecule, while it is not detectable from conductivity and $I-V$ characteristics. The obtained results imply that pristine and doped BlueP systems are encouraging alternatives for gas detection and should be investigated further for future gas sensing applications.

COMPUTATIONAL METHODS

In this study, through performing first-principles calculations based on DFT as executed in the Spanish Initiative for Electronic Simulations with Thousands of Atoms (SIESTA) package,[35] we have investigated the electronic structures and optical properties of blue phosphorene. The generalized gradient approximation (GGA) with the Perdew–Burke–Ernzerhof (PBE) exchange–correlation functional and the double ζ polarization (DZP) basis set are employed.[36] Moreover, the DFT-D2 method of Grimme is applied to account for van der Waals interactions.[37] All calculations are performed at a mesh cutoff energy of 150 Ry. For simulation of pristine and doped BlueP systems, a 3×3 rectangular supercell including 36 atoms is employed, as depicted in Figure 1. For geometry optimization, the relaxation of all atoms in the supercell is continued until the force on each atom is less than 0.01 eV $Å^{-1}$. To simulate pristine and doped BlueP, a 3×3 rectangular supercell with 36 atoms is employed, as depicted in Figure 1. The k-point sampling of $1 \times 3 \times 3$ is sufficient for geometry optimization. This k-grid is set to $1 \times 9 \times 9$ for the electronic structure and optical calculations. Because of paramagnetic gas molecules (NO and NO_2), spin polarization is regarded in the DFT calculations. The nonequilibrium Green's function (NEGF) formalism executed in the TRANSIESTA program package[38] is employed to study the transport properties. The $I-V$ characteristics are calculated through the Landauer–Buttiker method[39]

$$I(V_b) = G_0 \int_{\mu_L}^{\mu_R} T(E, V_b)\mathrm{d}E \quad (1)$$

where G_0 is the quantum conductance and $T(E,V_b)$ is the transmission coefficient of electrons incident at energy E under a bias voltage V_b. The difference between the two electrochemical potentials is eV_b.[9] For transmission spectrum analysis, the k-grid is adjusted to $1 \times 1 \times 100$. The adsorption energy (E_{ads}) is introduced to recognize the adsorption strength of the studied systems. E_{ads} can be defined as

$$E_{ads} = E_{BlueP+gas} - E_{BlueP} - E_{gas} + BSSE \quad (2)$$

where $E_{BlueP+gas}$, E_{BlueP}, and E_{gas} are the total energy of the fully relaxed system, the energy of the isolated substrate, and the energy of the isolated gas molecule, respectively. Furthermore, to remove the artificial attraction between the substrates and gas molecules, the basis set superposition error (BSSE) is deliberated.[40] Doping with different impurities induces different changes to BlueP's charge transfer. As a consequence, the Mulliken charge analysis is employed to calculate the charge transfer between substrates and gas molecules. The adsorption distance, d, is the distance between the vertical coordinate of the substrate and the gas molecule (see Table 1). The negative value of charge transfer shows electron transfer from the gas molecule to the substrate, while the positive value of charge transfer represents electron transfer from the substrate to the gas molecule.[23] To have a more detailed understanding of the interactions between the considered gas molecules and substrates, we plot the planar average charge density difference along the vertical direction in Figures 2 and 3.

https://doi.org/10.1021/acsomega.1c01898
ACS Omega 2021, 6, 18770−18781

AUTHOR INFORMATION

Corresponding Author

Mahdi Moradinasab − *Institute for Semiconductor Technology and Nanoelectronics, Technische Universität Darmstadt, Darmstadt 64289, Germany;* orcid.org/0000-0001-6689-5191; Email: m.moradinasab@gmail.com

Authors

Fatemeh Safari − *Department of Electrical Engineering, Dezful Branch, Islamic Azad University, Dezful, Iran*

Udo Schwalke − *Institute for Semiconductor Technology and Nanoelectronics, Technische Universität Darmstadt, Darmstadt 64289, Germany*

Lado Filipovic − *Institute for Microelectronics, Technische Universität Wien, Vienna 1040, Austria;* orcid.org/0000-0003-1687-5058

Complete contact information is available at: https://pubs.acs.org/10.1021/acsomega.1c01898

Notes

The authors declare no competing financial interest.

ACKNOWLEDGMENTS

This research work was supported by the Deutsche Forschungsgemeinschaft within the PARFAIT project (DFG 326384402).

REFERENCES

(1) Sarkar, D.; Gossner, H.; Hansch, W.; Banerjee, K. Tunnel-field-effect-transistor based gas-sensor: Introducing gas detection with a quantum-mechanical transducer. *Appl. Phys. Lett.* **2013**, *102*, No. 023110.

(2) Donarelli, M.; Ottaviano, L. 2D materials for gas sensing applications: A review on Graphene Oxide, MoS_2, WS_2 and Phosphorene. *Sensors* **2018**, *18*, 3638−3683.

(3) Tyagi, D.; Wang, H.; Huang, W.; Hu, L.; Tang, Y.; Guo, Z.; Ouyang, Z.; Zhang, H. Recent advances in two-dimensional-material-based sensing technology toward health and environmental monitoring applications. *Nanoscale* **2020**, *12*, 3535−3559.

(4) Noei, M.; Moradinasab, M.; Fathipour, M. A computational study of ballistic graphene nanoribbon field effect transistors. *Phys. E* **2012**, *44*, 1780−1786.

(5) Moradinasab, M.; Pourfath, M.; Fathipour, M.; Kosina, H. Numerical Study of Graphene Superlattice-Based Photodetectors. *IEEE Trans. Electron Devices* **2015**, *62*, 593−600.

(6) Perera, M. M.; Lin, M.-W.; Chuang, H.-J.; Chamlagain, B. P.; Wang, C.; Tan, X.; Cheng, M. M.-C.; Tománek, D.; Zhou, Z. Improved carrier mobility in few-layer MoS_2 field-effect transistors with ionic-liquid gating. *ACS Nano* **2013**, *7*, 4449−4458.

(7) Akhtar, M.; Anderson, G.; Zhao, R.; Alruqi, A.; Mroczkowska, J. E.; Sumanasekera, G.; Jasinski, J. B. Recent advances in synthesis, properties, and applications of phosphorene. *npj 2D Mater. Appl.* **2017**, *1*, No. 046101.

(8) Liu, H.; Neal, A. T.; Zhu, Z.; Luo, Z.; Xu, X.; Tománek, D.; Ye, P. D. Phosphorene: an unexplored 2D semiconductor with a high hole mobility. *ACS Nano* **2014**, *8*, 4033−4041.

(9) Kou, L.; Chen, C.; Smith, S. C. Phosphorene: Fabrication, properties, and applications. *J. Phys. Chem. Lett.* **2015**, *6*, 2794−2805.

(10) Zeng, J.; Cui, P.; Zhang, Z. Half layer by half layer growth of a blue Phosphorene monolayer on a GaN(001) substrate. *Phys. Rev. Lett.* **2017**, *118*, No. 046101.

(11) Zhu, Z.; Tománek, D. Semiconducting layered blue phosphorus: A computational study. *Phys. Rev. Lett.* **2014**, *112*, No. 176802.

(12) Zhang, J. L.; Zhao, S.; Han, C.; Wang, Z.; Zhong, S.; Sun, S.; Guo, R.; Zhou, X.; Gu, C. D.; Yuan, K. D.; Li, Z.; Chen, W. Epitaxial growth of single layer Blue Phosphorus: A new phase of two-dimensional phosphorus. *Nano Lett.* **2016**, *16*, 4903−4908.

(13) Xiao, J.; Long, M.; Deng, C.-S.; He, J.; Cui, L.-L.; Xu, H. Electronic Structures and Carrier Mobilities of Blue Phosphorus Nanoribbons and Nanotubes: A First-Principles Study. *J. Phys. Chem. C* **2016**, *120*, 4638−4646.

(14) Radisavljevic, B.; Radenovic, A.; Brivio, J.; Giacometti, V.; Kis, A. Single-Layer MoS_2 Transistors. *Nat. Nanotechnol.* **2011**, *6*, 147−150.

(15) Safari, F.; Fathipour, M.; Goharrizi, A. Y. Electronic and transport properties of blue phosphorene in presence of point defects: A first-principles study. *Phys. E* **2020**, *118*, No. 113938.

(16) Bolotsky, A.; Butler, D.; Dong, C.; Gerace, K.; Glavin, N. R.; Muratore, C.; Robinson, J. A.; Ebrahimi, A. Two-Dimensional Materials in Biosensing and Healthcare: From in Vitro Diagnostics to Optogenetics and beyond. *ACS Nano* **2019**, *13*, 9781−9810.

(17) Du, J.; Jiang, G. First-principle study on monolayer and bilayer SnP_3 sheets as the potential sensors for NO_2, NO, and NH_3 detection. *Nanotechnology* **2020**, *31*, No. 325504.

(18) Kou, L.; Frauenheim, T.; Chen, C. Phosphorene as a Superior Gas Sensor: Selective Adsorption and Distinct IV Response. *J. Phys. Chem. Lett.* **2014**, *5*, 2675−2681.

(19) Safari, F.; Fathipour, M.; Goharrizi, A. Y. Tuning electronic, magnetic, and transport properties of blue phosphorene by substitutional doping: A first-principles study. *J. Comput. Electron.* **2018**, *17*, 499−513.

(20) Luo, H.; Meng, R.; Gao, H.; Sun, X.; Xiao, J.; Ye, H.; Zhang, G.; Chen, X. First-principles study of nitric oxide sensor based on Blue Phosphorus monolayer. *IEEE Electron Device Lett.* **2017**, *38*, 1139−1142.

(21) Safari, F.; Moradinasab, M.; Fathipour, M.; Kosina, H. Adsorption of the NH_3, NO, NO_2, CO_2, and CO gas molecules on blue phosphorene: A first-principles study. *Appl. Surf. Sci.* **2019**, *464*, 153−161.

(22) Cheng, Y.; Meng, R.; Tan, C.; Chen, X.; Xiao, J. Selective gas adsorption and IV response of monolayer boron phosphide introduced by dopants: A first-principle study. *Appl. Surf. Sci.* **2018**, *427*, 176−188.

(23) Liu, N.; Zhou, S. Gas adsorption on monolayer blue phosphorus: implications for environmental stability and gas sensors. *Nanotechnology* **2017**, *28*, No. 175708.

(24) Salmankurt, B.; Gürel, H. H. In *Modifying of Gas Adsorption on Phosphorene*, AIP Conference Proceedings; AIP Publishing LLC, 2017; pp 120007.

(25) Sun, M.; Tang, W.; Ren, Q.; Wang, S. K.; Yu, J.; Du, Y. A first-principles study of light non-metallic atom substituted blue phosphorene. *Appl. Surf. Sci.* **2015**, *356*, 110−114.

(26) Sun, M.; Hao, Y.; Ren, Q.; Zhao, Y.; Du, Y.; Tang, W. Tuning electronic and magnetic properties of blue phosphorene by doping Al, Si, As and Sb atom: A DFT calculation. *Solid State Commun.* **2016**, *242*, 36−40.

(27) Li, T.; He, C.; Zhang, W. A novel porous C_4N_4 monolayer as a potential anchoring material for lithiumsulfur battery design. *J. Mater. Chem. A* **2019**, *7*, 4134−4144.

(28) Hellman, A.; Gronbeck, H. First-Principles studies of NO_x chemistry on Ag_n/α-Al_2O_3. *J. Phys. Chem. C* **2009**, *113*, 3674−3682.

(29) Liu, C.; Liu, C.-S.; Yan, X. Arsenene as a promising candidate for NO and NO_2 sensor: a first-principles study. *Phys. Lett. A* **2017**, *381*, 1092−1096.

(30) Pyykkö, P.; Atsumi, M. Molecular single-bond covalent radii for elements 1-118. *Chem. - Eur. J.* **2009**, *15*, 186−197.

(31) Hodgkinson, J.; Tatam, R. P. Optical gas sensing: A review. *Meas. Sci. Technol.* **2012**, *24*, No. 012004.

(32) Nayeri, M.; Moradinasab, M.; Fathipour, M. The transport and optical sensing properties of MoS_2, $MoSe_2$, WS_2 and WSe_2 semiconducting transition metal dichalcogenides. *Semicond. Sci. Technol* **2018**, *33*, No. 025002.

(33) Yaseen, M. S.; Murtaza, G.; Khalil, R. A. First principle study of structural, electronic, optical, and transport properties of ternary compounds $NaGaX_2$ (X=S,Se, and Te) in tetragonal chalcopyrite phase. *Opt. Quantum Electron.* **2019**, *51*, No. 367.

(34) Yu, P.; Cardona, M. *Fundamentals of Semiconductors: Physics and Materials Properties*; 4th ed.; Springer-Verlag: Berlin, Heidelberg, 2010.
(35) Soler, J. M.; Artacho, E.; Gale, J. D.; García, A.; Junquera, J.; Ordejón, P.; Sánchez-Portal, D. The SIESTA method for ab initio order- N materials simulation. *J. Phys. Condens. Matter* **2002**, *14*, 2745−2779.
(36) Perdew, J. P.; Burke, K.; Ernzerhof, M. Generalized gradient approximation made simple. *Phys. Rev. Lett.* **1996**, *77*, 3865−3868.
(37) Grimme, S. Semiempirical GGA-type density functional constructed with a long-range dispersion correction. *J. Comput. Chem.* **2006**, *27*, 1787−1799.
(38) Brandbyge, M.; Mozos, J. L.; P Ordejón, P.; Taylor, J.; Stokbro, K. Density-functional method for nonequilibrium electron transport. *Phys. Rev. B* **2002**, *65*, No. 165401.
(39) Topsakal, M.; Bagci, V. M. K.; Ciraci, S. Current-voltage ($I-V$) characteristics of armchair graphene nanoribbons under uniaxial strain. *Phys. Rev. B* **2010**, *81*, No. 205437.
(40) Abooali, A.; Safari, F. Adsorption and optical properties of H_2S, CH_4, NO, and SO_2 gas molecules on arsenene: a DFT study. *J. Comput. Electron.* **2020**, *9*, 1373−1379.

https://doi.org/10.1021/acsomega.1c01898
ACS Omega 2021, 6, 18770−18781